IAI Journals.ASM.org

Lack of Long-Lasting Hydrosalpinx in A/J Mice Correlates with Rapid but Transient Chlamydial Ascension and Neutrophil Recruitment in the Oviduct following Intravaginal Inoculation with *Chlamydia muridarum*

Hongbo Zhang,[a,d] Zhou Zhou,[a] Jianlin Chen,[a,d] Ganqiu Wu,[a,d] Zhangsheng Yang,[a] Zhiguang Zhou,[d] Joel Baseman,[a] Jin Zhang,[c] Robert Lee Reddick,[b] Guangming Zhong[a]

Departments of Microbiology and Immunology[a] and Pathology,[b] University of Texas Health Science Center at San Antonio, San Antonio, Texas, USA; Department of Pathology, Metropolitan Methodist Hospital, San Antonio, Texas, USA[c]; Departments of Pathology, Obstetrics and Gynecology, and Medicine, Second Xiangya Hospital, Department of Histology, Xiangya Medical School, Central South University, Changsha, Hunan, China[d]

Lower genital tract infection with *Chlamydia trachomatis* and *C. muridarum* can induce long-lasting hydrosalpinx in the upper genital tract of women and female mice, respectively. However, A/J mice were highly resistant to induction of long-lasting hydrosalpinx by *C. muridarum*. We further compared host inflammatory responses and chlamydial infection courses between the hydrosalpinx-resistant A/J mice and CBA/J mice known to be susceptible to hydrosalpinx induction. Both mouse strains developed robust pyosalpinx during the acute phase followed by hydrosalpinx during the chronic phase. However, the hydrosalpinges disappeared in A/J mice by day 60 after infection, suggesting that some early hydrosalpinges are reversible. Although the overall inflammatory responses were indistinguishable between CBA/J and A/J mice, we found significantly more neutrophils in oviduct lumen of A/J mice on days 7 and 10, which correlated with a rapid but transient oviduct invasion by *C. muridarum* with a peak infection on day 7. In contrast, CBA/J mice developed a delayed and extensive oviduct infection. These comparisons have revealed an important role of the interactions of oviduct infection with inflammatory responses in chlamydial induction of long-lasting hydrosalpinx, suggesting that a rapid but transient invasion of oviduct by chlamydial organisms can prevent the development of the long-lasting hydrosalpinges.

Long-lasting hydrosalpinx is a pathological hallmark of tubal factor infertility associated with *Chlamydia trachomatis* infection in women (1) and *C. muridarum* infection in female mice (2–4). The precise mechanism of *Chlamydia*-induced long-lasting hydrosalpinx remains unknown, although *Chlamydia*-triggered inflammatory responses have been hypothesized to contribute significantly to chlamydial pathogenesis (5, 6). For example, it is not clear whether live organism infection in the fallopian tube is necessary for induction of hydrosalpinx, how chlamydial organisms trigger hydrosalpinx-causing inflammation, and when hydrosalpinx becomes irreversible. Since it is difficult to directly address these questions during *C. trachomatis* infection in women, a murine model of *C. muridarum* infection has been used extensively to study pathogenic mechanisms and immune responses of *C. trachomatis* (7, 8). This is because genital tract infection of mice with *C. muridarum* can lead to long-lasting hydrosalpinx that closely mimics hydrosalpinx found in *C. trachomatis*-infected women under laparoscopy (9–11).

To delineate the host inflammatory mechanism of chlamydial induction of long-lasting hydrosalpinx, Shah et al. carefully compared the genital tract inflammatory pathological responses between the chlamydial infection-resistant C57BL/6J and the susceptible C3H/HeN mice, which led the authors to correlate a robust acute inflammatory response with the development of long-lasting hydrosalpinx observed on day 56 after infection (3). However, it is not known whether the intensity of the acute inflammatory response can always contribute to chlamydial induction of long-lasting hydrosalpinx, since both C57BL/6L and C3H/HeN can develop significant long-lasting hydrosalpinx, although with different incidence rates (3, 12). It is also unclear whether live organism infection in the oviduct is necessary for sustaining hydrosalpinx-causing inflammation, since live organism recovery was monitored in the lower but not upper genital tract (3). Darville et al. further reported that mice deficient in TLR2 failed to develop a robust acute inflammatory response with decreased oviduct dilation (13). However, these observations were made under a microscope on day 35 after infection (13). It is not clear whether the proposed TLR2-mediated signaling pathway is sufficient for *C. muridarum* induction of long-lasting hydrosalpinx. More importantly, the TLR2 knockout mice developed an equivalent level of chronic inflammation in the oviduct on day 35 after infection (13), and mice deficient in MyD88, a critical adaptor molecule of the TLR2-mediated signaling pathway, developed more severe long-lasting hydrosalpinx (14). These findings question the role of TLR2 signaling pathways in chlamydial induction of long-lasting hydrosalpinx. The role of neutrophils in chlamydial infection and pathogenesis has been extensively studied. While some found a protective role of early neutrophil infiltration in protection against chlamydial pathogenicity (15, 16), others correlated an increased infiltration of neutrophils with chlamydial pathogenic-

Received 11 January 2014 **Returned for modification** 31 January 2014
Accepted 26 March 2014
Published ahead of print 7 April 2014
Editor: R. P. Morrison
Address correspondence to Guangming Zhong, Zhongg@UTHSCSA.EDU.
Copyright © 2014, American Society for Microbiology. All Rights Reserved.
doi:10.1128/IAI.00055-14

ity (17). Many other host molecules have been shown to contribute to chlamydial pathogenicity in the upper genital tract, including matrix metalloproteinases (18), inducible nitric oxide synthase (19), interleukin-1 (IL-1) receptor (20), caspase-1 (6, 21), IL-17 (16), CD28 (22), and tumor necrosis factor alpha (TNF-α) (23). However, none of these previous studies have sufficiently addressed the questions on the mechanism, location, duration, and extent of inflammatory signaling pathways activated during chlamydial infection as they influence chlamydial induction of long-lasting hydrosalpinx. Recently, we correlated the live organism infection in the oviduct with chlamydial induction of long-lasting hydrosalpinx (12), which is consistent with the observation that epithelial cells actively infected with chlamydial organisms are more inflammatory than cells stimulated with noninfectious chlamydial antigens (5, 24, 25). The current study extends our previous observations by further defining the relationship between oviduct infection and oviduct inflammatory responses in chlamydial pathogenesis.

In the current study, we unexpectedly found that A/J mice were highly resistant to induction of long-lasting hydrosalpinx by *C. muridarum*. We took advantage of this mouse property and carefully compared its host inflammatory responses and chlamydial infection courses with that of CBA/J mice that are known to be susceptible to hydrosalpinx induction (12). We found that both mouse strains developed robust pyosalpinx during the acute phase followed by hydrosalpinx during the chronic phase. However, in A/J mice, the hydrosalpinges disappeared by day 60 after infection, demonstrating that some early hydrosalpinges are reversible. Although the overall inflammatory responses were indistinguishable between CBA and A/J mice, an accelerated exudation of neutrophils into the oviduct lumen coupled with a rapid but transient oviduct infection within the first week after intravaginal inoculation was identified in the hydrosalpinx-resistant A/J mice. In contrast, a more extensive oviduct infection beyond 2 weeks after intravaginal inoculation was found in the hydrosalpinx-susceptible CBA/J mice. These observations have revealed an important relationship between oviduct infection and inflammatory responses in chlamydial induction of long-lasting hydrosalpinx, correlating a rapid but transient invasion of oviduct by chlamydial organisms followed by an enhanced neutrophil exudation with the prevention of the irreversible hydrosalpinges.

MATERIALS AND METHODS

Chlamydial organisms and infection. *Chlamydia muridarum* (Nigg strain) organisms used in the current study were propagated in HeLa cells (human cervical carcinoma epithelial cells; ATCC catalog no. CCL2.1), purified, aliquoted, and stored as described previously (26). Female CBA/J (stock number 000656) and A/J mice (000646) were purchased at the age of 5 to 6 weeks old from Jackson Laboratories (Bar Harbor, ME). Each mouse was inoculated intravaginally with 2×10^5 inclusion-forming units (IFUs) of *C. muridarum* organisms in 20 μl of SPG (sucrose-phosphate-glutamate buffer). Five days prior to infection, each mouse was injected subcutaneously with 2.5 mg depot medroxyprogesterone acetate (Depo-Provera; Pharmacia Upjohn, Kalamazoo, MI) to synchronize the estrus cycle and increase mouse susceptibility to chlamydial infection. For *in vitro* infection of HeLa cells, HeLa cells grown on coverslips in 24-well plates containing Dulbecco's modified Eagle medium (DMEM) (GIBCO BRL, Rockville, MD) with 10% fetal calf serum (FCS; GIBCO BRL) at 37°C in an incubator supplied with 5% CO_2 were inoculated with *C. muridarum* organisms as described previously (6). The infected cultures were examined by immunofluorescence as described below.

Monitoring live *C. muridarum* organism recovery from swabs and genital tract tissues. To monitor live organism shedding, vaginal swabs were taken on different days after intravaginal infection. Each swab was suspended in 500 μl of ice-cold SPG followed by vortexing with glass beads, and the released organisms were titrated on HeLa cell monolayers in duplicates as described previously (14). To monitor upper genital tract infection, the genital tract tissue was harvested sterilely from each mouse on different days after infection as indicated in individual experiments. Each tissue was cut into 3 segments, including vagina/cervix, uterus/uterine horn (both sides from the same mouse were combined as a single segment), and oviducts/ovaries (both sides from the same mouse were pooled as a single tissue sample). Each segment sample was homogenized in 300 μl of SPG using a 2-ml mini tissue grinder (Fisher Scientific, Pittsburgh, PA). After brief sonication, the released live organisms were titrated as described above. The total number of IFUs per swab/tissue was calculated based on the number of IFUs per field, number of fields per coverslip, dilution factors, and inoculation and total sample volumes. An average was taken from the serially diluted and duplicate samples for any given swab/tissue. The calculated total number of IFUs/swab or tissue was converted into $\log_{10}$ values, and the $\log_{10}$ IFUs were used to calculate means and standard deviations for each group at each time point.

Evaluating mouse genital tract tissue pathologies and histological scoring. Mice were sacrificed on different days postinfection as indicated in individual experiments, and urogenital tract tissues were isolated. Before the tissues were removed, *in situ* gross examination was performed for evidence of oviduct pathologies, including pyosalpinx and hydrosalpinx. Mice with pyosalpinx or hydrosalpinx on either side of oviducts were determined to be positive when calculating the percentage of mice with positive oviduct pathology. The severity of hydrosalpinx was scored based on the following criteria: 0, no pyosalpinx or hydrosalpinx; 1, pyosalpinx or hydrosalpinx barely visible, requiring confirmation under stereoscope or microscope examination; 2, pyosalpinx or hydrosalpinx clearly visible by the naked eye but smaller in size than the ovary on the same side; 3, pyosalpinx or hydrosalpinx size equal to that of the ovary on the same side; and 4, pyosalpinx or hydrosalpinx size larger than that of the ovary on the same side. Scores from both sides of oviducts from the same mouse were combined as the score for that mouse. Obviously, both hydrosalpinx incidence rates and hydrosalpinx severity scores were determined by the naked eye by observing the isolated genital tract organs. Thus, they represent gross pathology.

For histological scoring and inflammatory cell counting, the excised mouse genital tract tissues, after photographing, were fixed in 10% neutral formalin, embedded in paraffin, and serially sectioned longitudinally (with 5 μm/each section). Efforts were made to include cervix, both uterine horns, and oviducts, as well as lumenal structures of each tissue in each section. The sections were stained with hematoxylin and eosin (H&E) as described elsewhere (3). The H&E-stained sections were scored for severity of inflammation and pathologies based on the modified schemes established previously (3, 14) by board-certified pathologists who were blinded as to mouse group designation. The following values were used for scoring the dilatation of the oviduct: 0, no significant dilatation; 1, mild dilatation of a single cross-section; 2, one to three dilated cross-sections; 3, more than three dilated cross-sections; and 4, confluent pronounced dilation. Inflammatory cell infiltrates were scored for oviduct lumen and interstitial tissue (oviduct wall tissue) separately: 0, no significant infiltration; 1, infiltration at a single focus; 2, infiltration at two to four foci; 3, infiltration at more than four foci; and 4, confluent infiltration. Scores from both sides of the oviducts were added to represent the oviduct pathology for a given mouse, and the individual mouse scores were calculated as medians for each group. Thus, oviduct lumenal dilation scores and oviduct lumen or wall tissue inflammation scores represent microscopic observations. Together with the gross pathology parameters hydrosalpinx incidence and severity, the combination of the 4 parameters allow us to more accurately describe the oviduct pathology.

In some experiments, the individual inflammatory cells were identi-

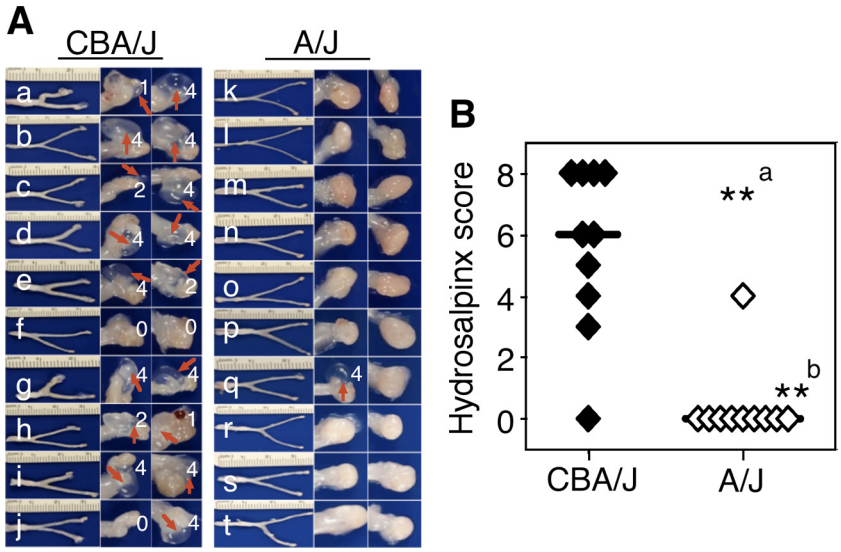

FIG 1 Development of long-lasting hydrosalpinx in CBA/J but not A/J mice following *C. muridarum* infection. Both CBA/J ($n = 10$) and A/J ($n = 10$) mice were intravaginally infected with 2×10^3 IFUs of *C. muridarum*, and 60 days after infection all mice were sacrificed for observing hydrosalpinx. (A) Images of whole genital tracts from all 20 mice are presented in the left columns (a to j for CBA/J, k to t for A/J) with vagina on the left and oviduct/ovary on the right sides. The images for areas covering the oviduct/ovary portions were magnified and are shown to the right of the corresponding whole-genital-tract images, with hydrosalpinx marked with red arrows and hydrosalpinx severity scores indicated in white numbers. (B) The hydrosalpinx severity scores and incidence rates (data not shown) are listed along the *y* axis. Mice with hydrosalpinx in either or both oviducts were considered positive for hydrosalpinx. The severity of both hydrosalpinges from a given mouse was scored separately and added together as the severity score assigned to the particular mouse. Note that A/J mice failed to develop any significant hydrosalpinx, with both hydrosalpinx incidence (a, Fisher's exact test) and severity (b, Wilcoxon rank-sum test) significantly lower than those of CBA/J mice (**, $P < 0.01$ for both).

fied and counted from oviduct lumenal and wall tissue areas. For example, both total inflammatory cells and neutrophils and mononuclear cells were counted in individual 100× objective lens views. Inflammatory cells from 5 to 10 random 100× objective lens views were counted from each oviduct cross-section from both sides. An average number of total and individual inflammatory cells per view from each mouse was used to calculate mouse group means and standard deviations.

Immunofluorescence assay. HeLa cells grown on coverslips with chlamydial infection were fixed and permeabilized for immunostaining as described previously (27, 28). Hoechst dye (blue; Sigma) was used to visualize nuclear DNA. For titrating IFUs from swab and tissue homogenate samples, a mouse antichlamydial lipopolysaccharide (LPS) antibody (clone MB5H9; unpublished observations) plus a goat anti-mouse IgG conjugated with Cy3 (red; Jackson ImmunoResearch Laboratories, Inc., West Grove, PA) were used to visualize chlamydial inclusions. Hoechst dye (Sigma-Aldrich, St. Louis, MO) was used to label DNA (blue). For detecting *C. muridarum* inclusions in mouse genital tract tissue sections, a rabbit anti-*C. muridarum* antibody (raised with purified *C. muridarum* elementary bodies; unpublished data) was used to label chlamydial inclusions followed by a goat anti-rabbit IgG conjugated with Cy2 (green; Jackson ImmunoResearch Laboratories, Inc.). All immunofluorescence-labeled samples were observed under an Olympus AX-70 fluorescence microscope (Olympus, Melville, NY). The images were taken using a Simple PCI and processed using Adobe Photoshop as described previously (29, 30).

Statistical analyses. The differences in IFUs recovered from mouse swabs and tissues and differences in inclusion and inflammatory cell counting were analyzed using Kruskal-Wallis or analysis of variance (ANOVA) followed by Student *t* test. The pathology scores (both gross and microscopic) were analyzed with a Wilcoxon rank-sum test. Fisher's exact test was used to analyze category data, including incidence rates.

RESULTS

Failure of A/J mice to develop long-lasting hydrosalpinx following *C. muridarum* intravaginal infection. We previously reported that five strains of mice, including CBA/J, were induced to develop long-lasting hydrosalpinx upon intravaginal infection with *C. muridarum* (12). When we tested A/J mice, the result was unexpected. The A/J mice were highly resistant to hydrosalpinx induction (Fig. 1). With CBA/J mice as a control, both strains ($n = 10$ for CBA/J and $n = 10$ for A/J) were sacrificed for observing hydrosalpinx on day 60 after intravaginal infection with *C. muridarum*. A/J mice failed to develop any significant long-lasting hydrosalpinx. Both hydrosalpinx incidence rates (Fisher's exact test) and severity scores (Wilcoxon rank-sum test) were significantly lower in A/J than CBA/J mice ($P < 0.01$ for both).

Early pyohydrosalpinges in both CBA/J and A/J but long-lasting hydrosalpinx only in CBA/J mice. To investigate the mechanism of *Chlamydia*-induced hydrosalpinx, we compared oviduct gross pathology following *C. muridarum* infection in both CBA/J and A/J mice (Fig. 2). Mice infected with *C. muridarum* were sacrificed for visual observation of pyosalpinx and hydrosalpinx on days 3, 7, 10, 14, 21, 28, 35, and 60 after infection. Pyosalpinx and hydrosalpinx were visually identified in both CBA/J and A/J mice. These gross pathologies were validated under a microscope. Oviducts with pyosalpinx were filled with inflammatory infiltrates, while those with hydrosalpinx showed empty lumenal space suggestive of clear solution accumulation. Note that inflammation infiltration was also observed under microscopy in some oviducts without visually detectable pathology. Obviously, microscopic observation is more sensitive than visual observation. No oviduct gross pathology was detected in mice sacrificed on days 3 and 7. Thus, images from these 2 time points were not included. Both the gross pathology incidence rates and severity scores were determined for each mouse and calculated from each group at each time point (Fig. 3). Extensive pyosalpinx was observed in

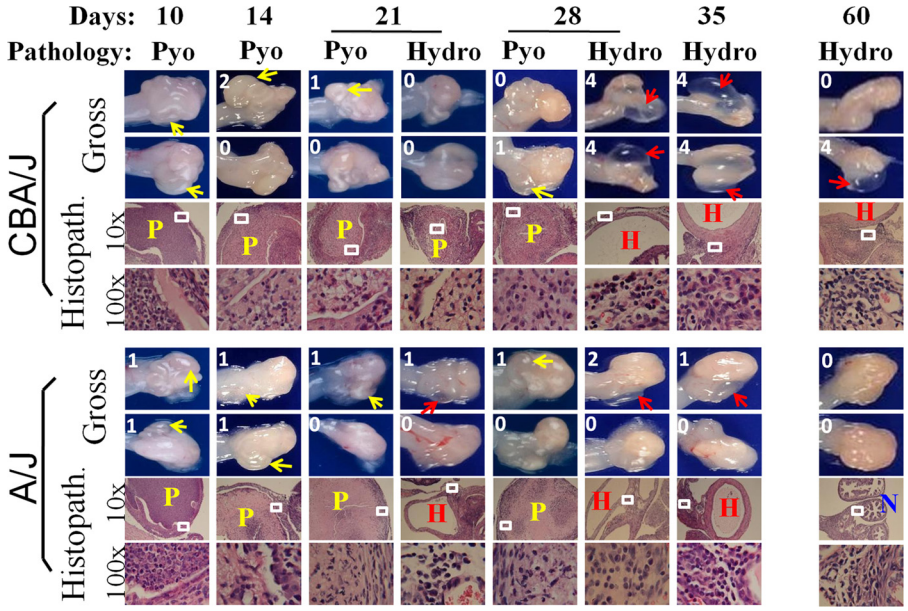

FIG 2 Monitoring oviduct gross pathology along *C. muridarum* infection course. CBA/J and A/J mice were infected with *C. muridarum* as described in the legend to Fig. 1 and sacrificed for visual observation of oviduct pathology, including both pyosalpinx and hydrosalpinx, on days 3 ($n = 5$ for CBA/J and A/J groups, respectively), 7 ($n = 5$), 10 ($n = 6$), 14 ($n = 5$), 21 ($n = 5$), 28 ($n = 5$), 35 ($n = 5$), and 60 ($n = 10$) after inoculation. One or two representative images of oviduct/ovary from both sides of a mouse genital tract are presented for both strains of mice at each time point, except for days 3 and 7 (no gross pathology could be detected on these early days). The visually observable pyosalpinx (Pyo) was marked with yellow and hydrosalpinx (Hydro) with red arrows, while the gross pathology severity was scored according to the criteria described in Materials and Methods and marked with numbers in white in corresponding images. To validate the visually observable gross pathology, H&E-stained sections were prepared from the corresponding genital tract tissues (Histopath.). Representative images from each strain of mice, taken under a 10× and 100× objective lens, respectively, are shown with pyosalpinx, hydrosalpinx, or normal oviducts marked with P (in yellow), H (red), or N (blue), respectively. White rectangles in images of a 10× objective lens indicate the areas where the images were further magnified under the 100× objective lens. Note that oviducts with pyosalpinx (yellow P) were filled with inflammatory infiltrates, while those with hydrosalpinx (red H) showed empty lumenal space suggestive of clear solution accumulation. Inflammation was also observed under microscopy in oviducts without visually detectable pathology.

both strains of mice during the first 4 weeks after infection, followed by or overlapping hydrosalpinx in both strains of mice. However, by day 60, no significant hydrosalpinx was detected in A/J mice.

Rapid neutrophil recruitment into oviduct lumen of A/J during acute phase. We first compared the overall inflammatory infiltration in oviduct lumen and tissues separately between CBA/J and A/J mice (Fig. 4). The inflammatory scores were largely similar between these two strains of mice along the entire infection course. The oviduct lumenal inflammatory scores peaked on day 14, while the tissue scores peaked on days 10 and 14 after infection. The only significant differences between CBA/J and A/J mice were the tissue inflammatory scores on day 60. There was no overall significant difference. These observations suggest that the microscopic assessment of overall inflammation infiltration was not sensitive enough for identifying correlates associated with either hydrosalpinx resistance or susceptibility.

We then counted individual types of inflammatory cells, including neutrophils and mononuclear cells (mainly consisting of macrophages, lymphocytes, and plasma cells), in both oviduct lumen and tissue sections (Fig. 5). Under a 100× objective lens, neutrophils and mononuclear cells can be distinguished. We found that during the first 10 days of infection, most inflammatory cells from either oviduct lumen or tissue sections were neutrophils for both CBA/J and A/J mice. Interestingly, the level of neutrophil exudation in the oviduct lumen was significantly higher in the hydrosalpinx-resistant A/J than the susceptible CBA/J mice on both days 7 and 10. The tissue neutrophil infiltration peaked on day 7, while the lumenal neutrophils peaked on day 10. By day 14, the neutrophils started to drop and continued to decline thereafter, which marked the onset of chronic infection. Consistent with the chronic infection, significant numbers of inflammatory cells became mononuclear cells on day 14. The mononuclear cells continued to increase and peaked on day 28. By day 60, only a minimal number of inflammatory cells was detected in A/J mice, while a significant number of inflammatory cells was still maintained in CBA/J mice, which is consistent with the overall inflammation assessment described above for Fig. 4. Together, the above-described observations demonstrated that the hydrosalpinx-resistant A/J mice responded to chlamydial infection with a more rapid recruitment of neutrophils into the oviduct lumen during the acute phase with significantly more neutrophil infiltration on days 7 and 10 after infection compared to those of the hydrosalpinx-susceptible CBA/J mice. These results suggested a correlation between rapid neutrophil recruitment during the acute phase and lack of long-lasting hydrosalpinx.

Oviduct infection peaks earlier but resolves faster in A/J than CBA/J mice. Since both infection courses and host responses can contribute to chlamydial induction of hydrosalpinx, we further compared chlamydial infection courses in CBA/J and A/J mice by monitoring the live organism recovery from vaginal swabs following intravaginal inoculation with *C. muridarum* (Fig. 6). We found that A/J mice displayed a significantly reduced infection time course. The level of live organisms recovered from A/J mouse

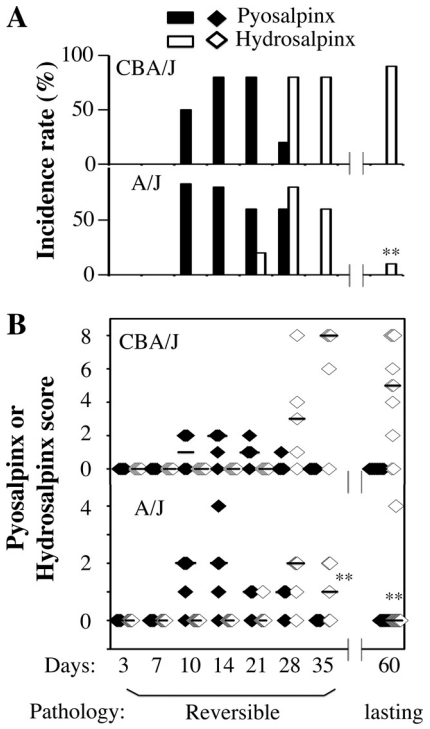

FIG 3 Scoring oviduct gross pathology along *C. muridarum* infection course. Both the gross pathology incidence rates (A) and severity scores (B) were calculated from each group of mice presented in Fig. 2. The values are listed along the *y* axis. Note that extensive pyosalpinx (solid bars or diamonds) was observed in both strains of mice during the first 4 weeks after infection followed by or overlapping hydrosalpinx (open bars or diamonds) in both strains of mice. However, by day 60, hydrosalpinx incidence was significantly higher in CBA/J mice (*, $P < 0.01$ by Fisher's exact; also see the legend to Fig. 1), and by days 35 and 60, hydrosalpinx severity was significantly lower in A/J mice (*, $P < 0.01$ by Wilcoxon rank-sum test).

vaginal swabs dropped significantly on day 14 compared to those of CBA/J mice. All 10 A/J mice cleared infection by day 35, while CBA mice continued to shed live organisms until day 56 after infection. Obviously, the reduced recovery of live organisms from vaginal swabs correlated well with the lack of hydrosalpinx in A/J mice.

However, the vaginal swab infectious organism recovery only measured infection of the lower genital tract, which might not reflect the extent of infection in the upper genital tract where long-lasting hydrosalpinx occurs. We then directly detected chlamydial infection in the upper genital tract (Fig. 7). Using an immunofluorescence assay, we detected significantly more inclusions in the oviduct sections of A/J than CBA/J mice on day 7 after infection. However, the number of inclusions rapidly increased so that those of A/J mice surpassed those of CBA/J mice on day 10 after infection and thereafter. By day 21, chlamydial inclusions were still detectable in the oviduct of CBA/J but not A/J mice. To validate this observation, we quantitated the infectious organisms recovered from oviduct/ovary tissue homogenates in independent experiments. We found that the level of infectious organisms was higher in A/J mice on day 7 but significantly lower on days 14 and 21 compared to levels for CBA/J mice. Infectious particles were still recovered from the oviduct/ovary tissue of CBA/J but not A/J mice by day 28 after infection when early hydrosalpinges became obvious (Fig. 2). These observations together have confirmed that the hydrosalpinx-resistant A/J mice experienced a rapid but transient oviduct infection while the hydrosalpinx-susceptible CBA/J mice developed a slower but more extended oviduct infection.

DISCUSSION

Our unexpected discovery of A/J mice as being highly resistant to induction of long-lasting hydrosalpinx by *C. muridarum* has pro-

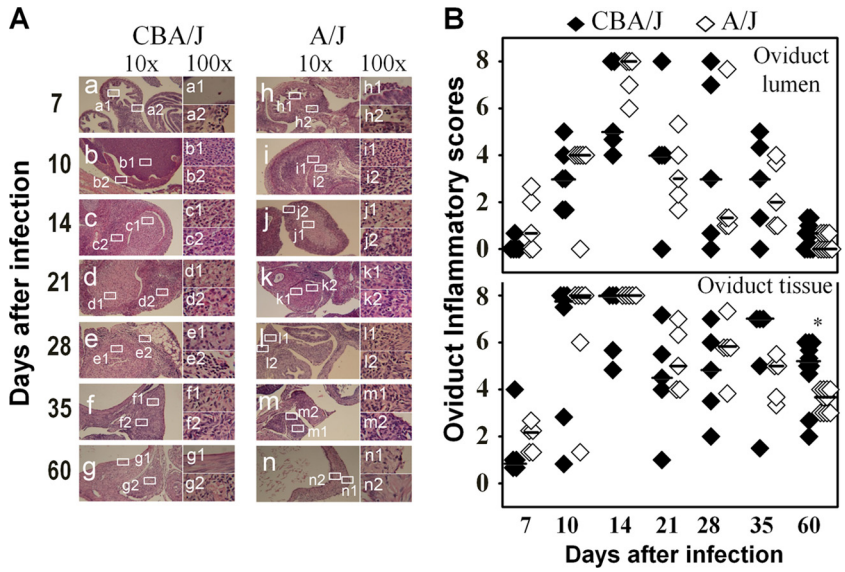

FIG 4 Monitoring oviduct inflammatory histopathology following *C. muridarum* infection. The same oviduct tissues from the experiments described for Fig. 2 were subjected to H&E staining for evaluating inflammatory histopathology. (A) Representative images from each group, taken under 10× (left column, a to g in CBA/J mice and h to n in A/J mice) and 100× objective lenses (right column, a1 to g1 and a2 to g2 in CBA/1J mice and h1 to n1 and h2 to n2 in A/J mice) are shown. White rectangles in images from the 10× objective lens indicate the same areas from which the right-side images were taken under a 100× objective lens. (B) The severity of inflammatory infiltration or exudation in oviduct tissue (bottom) and lumen (top) areas was scored separately as described in Materials and Methods and is listed along the *y* axis (solid diamonds for CBA/J, open diamonds for A/J). Note that both groups of mice developed extensive inflammatory histopathology that peaked on day 14 after infection in both oviduct tissue and lumen (*, $P < 0.05$ by Wilcoxon rank-sum test).

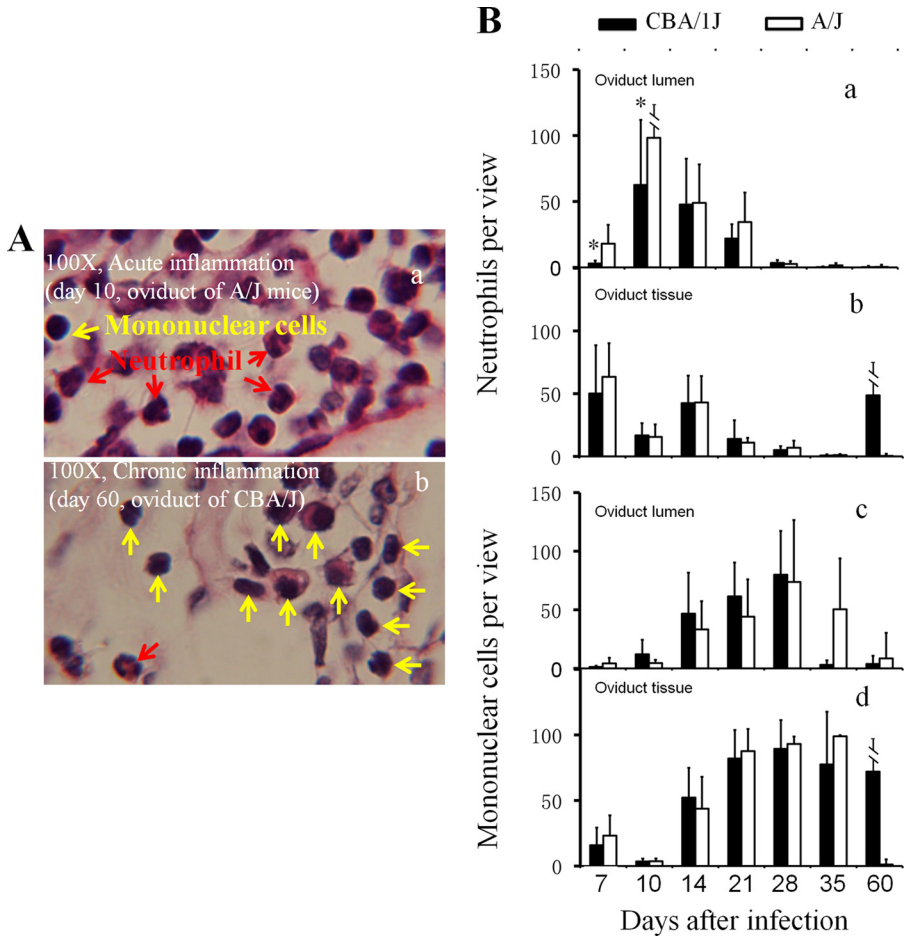

FIG 5 Detecting oviduct inflammatory cells following *C. muridarum* infection. The H&E-stained sections described in the legend to Fig. 4 were reexamined for identifying neutrophils and mononuclear cells. (A) Example images marked with either neutrophils (red arrows) or mononuclear cells (yellow arrows) are shown. In the image taken from an oviduct tissue section with an acute infection, more neutrophils were detected (a, A/J mice), while at the chronic stage, more mononuclear inflammatory cells, including plasma cells, lymphocytes, and macrophages, were detected (b, CBA/J mice). Total inflammatory cells and neutrophil and mononuclear cell subpopulations were counted in individual 100× objective lens views (for high-density infiltration) or the entire oviduct tissue or lumen section (for scarce infiltration). (B) The number of neutrophils (a and b) and mononuclear cells (c and d) per view from either oviduct lumen (a and c) or tissue (b and d) areas of each mouse was used to calculate means and standard deviations for each group as shown along the *y* axis. Note that both CBA/J (solid bar) and A/J (open bar) mice were dominated by neutrophils in both oviduct lumen and tissues during the first 10 days of infection (a and b), followed by mononuclear cells (c and d). Interestingly, levels of oviduct lumenal neutrophils were significantly higher in A/J than CBA/J mice on days 7 and 10.

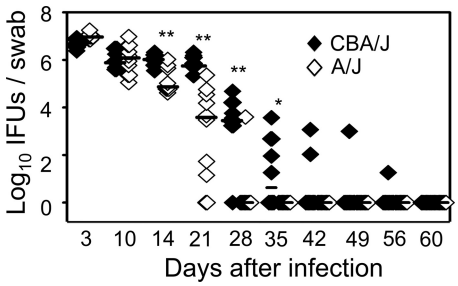

FIG 6 Monitoring *C. muridarum* intravaginal infection time course. The same CBA/J (solid diamonds) and A/J (open diamonds) mice intravaginally infected with *C. muridarum* as described in the legend to Fig. 1 were monitored for live organism recovery from vaginal swabs taken after infection as indicated along the *x* axis. Swab samples were titrated on HeLa cell monolayers, and the inclusion-forming units (IFUs) calculated from each group were expressed as $\log_{10}$ IFUs as shown along the *y* axis. Note that the hydrosalpinx-resistant A/J mice displayed a reduced level of live organism recovery and shortened shedding time course (*, $P < 0.05$; **, $P < 0.01$; Student *t* test).

vided us a unique tool for further investigating the mechanisms of chlamydial pathogenic mechanisms in the murine model. By simultaneously comparing host inflammatory responses and chlamydial infection courses between the hydrosalpinx-resistant A/J and CBA/J mice known to be susceptible to hydrosalpinx induction, we have further defined the relationship between oviduct infection and inflammatory responses in chlamydial pathogenesis. Although both mouse strains developed robust pyosalpinx during the acute phase followed by hydrosalpinx during the chronic phase, the hydrosalpinges disappeared in A/J mice by day 60 after infection. The lack of long-lasting hydrosalpinx in A/J mice correlated with an accelerated exudation of neutrophils into the oviduct lumen during early stages of infection. As a result, the A/J mice only experienced a transient oviduct infection. In contrast, the hydrosalpinx-susceptible CBA/J mice developed more extended mononuclear cell infiltration with a more extensive oviduct infection, which may significantly contribute to the development of long-lasting hydrosalpinx.

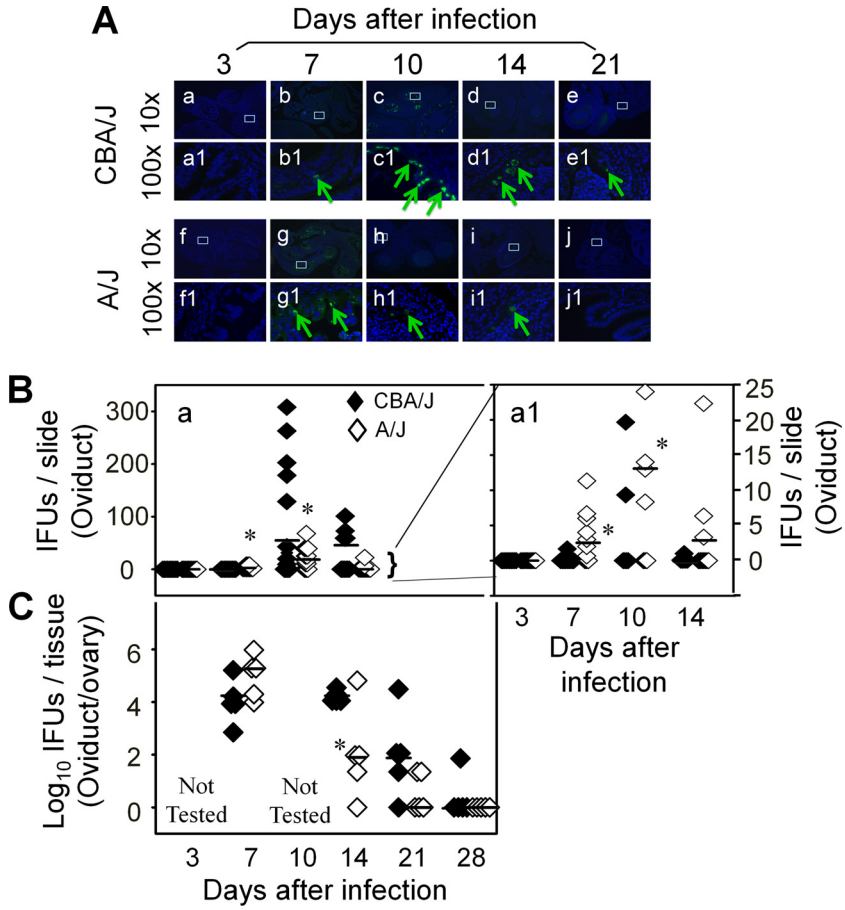

FIG 7 Monitoring oviduct infection following *C. muridarum* intravaginal inoculation. (A) The oviduct sections from genital tract tissues harvested from mice on days 3 ($n = 5$ for CBA/J and A/J mice, respectively), 7 ($n = 10$), 10 ($n = 10$), 14 ($n = 5$), and 21 ($n = 5$) after infection, as described in the legend to Fig. 2, plus additional mice for immunofluorescence assay. The sections were labeled with a DNA dye (blue) and a rabbit antichlamydial antibody (raised with *C. muridarum* elementary bodies; green). Representative images taken under 10× (a to j) and 100× (a1 to j1) magnification from both CBA/J (a to e and a1 to e1) and A/J (f to j and f1 to j1) at each time as indicated on top of each image are presented with representative inclusions marked with green arrows. White rectangles in images from a 10× objective lens indicate the same areas viewed under the 100× objective lens. (B) The inclusions were counted and semiquantitated as described in Materials and Methods, as shown along the *y* axis. The number of inclusions per slide varied considerably from 0 to >300 (image a). To show differences between the two groups of mice, the region covering samples with 25 or fewer inclusions was magnified as image a1. Note that on day 7 after infection, significantly more inclusions were detected in the oviduct sections of A/J mice (a1, open diamonds). The number of inclusions rapidly increased in CBA/J mice (solid), surpassing the A/J mice on day 10 postinfection or thereafter. (C) The microscopic observations described here were validated by titrating infectious chlamydial organisms from oviduct/ovary tissue homogenates harvested from mice on days 3, 7, 10, 14, 21, and 28, as indicated along the *x* axis. The recovered IFUs, expressed in $\log_{10}$ values, are shown along the *y* axis. Note that the IFUs were higher in A/J oviduct/ovary tissue samples on day 7 but significantly lower on days 14 and 21 (*, $P < 0.05$; Student *t* test). The IFU recovery study was carried out with 5 mice per group.

A second surprise finding in the current study was that the hydrosalpinx-resistant A/J mice also developed robust pyosalpinx and maintained hydrosalpinx during the first 5 weeks. More than 50% of A/J mice developed visible hydrosalpinx by days 28 or 35 after infection. This is certainly an underestimate, since visual observation is not nearly as sensitive as microscope examination for identifying hydrosalpinx. Microscopic examination of the same A/J mouse oviducts validated the hydrosalpinges visually identified. The hydrosalpinges revealed under microscopy were as severe as those previously identified microscopically on day 35 (13) or 42 (31) after infection. However, by day 60 after infection, most of these early hydrosalpinges disappeared in A/J mice. These observations have demonstrated that the hydrosalpinges detected using microscopy during the first 5 or 6 weeks of infection are reversible and do not always develop into long-lasting hydrosalpinx. Indeed, fibrosis is known to be reversible (32). Tubal fibrosis responsible for causing these early hydrosalpinges may be reversed in the late stages of infection. In addition, it has been reported that not all mouse hydrosalpinges represent complete fibrotic blockage of the oviducts (3). However, it is the long-lasting hydrosalpinx that is most medically relevant, since fallopian tubal occlusion is detected in most women with tubal-factor infertility by hysterosalpingography (33). Thus, it is necessary to ensure that the observed hydrosalpinx is long-lasting and represents irreversible tubal blockage when investigating chlamydial pathogenic mechanisms using the *C. muridarum* murine infection model, which can be achieved by either using a dye solution to directly measure the oviduct patency (3) or visually observing hydrosalpinx 60 days or longer after infection (12, 14, 22, 27, 34, 35).

A third surprise finding in the current manuscript was our observation that significantly more chlamydial inclusions in the oviduct sections and higher numbers of infectious organisms in

the homogenate of oviduct/ovary were detected in the hydrosalpinx-resistant A/J mice on day 7 after infection compared to CBA/J mice. This rapid ascension should have made the A/J mice more susceptible to the development of more severe upper genital pathology. Although the A/J mice developed pyosalpinx and maintained hydrosalpinx during the first 5 weeks, by day 60, these early hydrosalpinges disappeared. The question is why? One hypothesis is that the rapid ascension triggered an accelerated acute inflammation, as evidenced by the significantly enhanced neutrophil exudation into oviduct lumen of the A/J mice on days 7 and 10 after infection. The enhanced acute inflammatory neutrophils may be effective in limiting chlamydial infection in the oviduct. This hypothesis is supported by the finding that the rapid oviduct infection peaked on day 7, followed by a significantly suppressed chlamydial organism count on days 10 and 14 and no infectious organisms detectable by day 28. The roles of early neutrophil infiltration in protection against chlamydial infection and pathogenicity have been demonstrated previously (15, 16). Although the significantly reduced oviduct infection may have induced the acute pyosalpinx and early hydrosalpinx, it may not be able to maintain inflammation that drives the development of long-lasting hydrosalpinx. This hypothesis is also supported by our recent findings that long-lasting hydrosalpinx require significant and extended oviduct infection (12). Alternatively, a second hypothesis is that A/J mice are genetically defective in responding to chlamydial infection with a hydrosalpinx-causing prolonged inflammatory response, which is inconsistent with the equally robust pyosalpinx we detected in both A/J and CBA/J mice. Interestingly, A/J mice are known to be deficient in complement component 5 (C5) (36, 37). Since C5 has been found to play significant roles in various inflammatory pathologies and anti-C5 therapy has been shown to reduce the severity of autoimmune pathologies (38, 39), it is possible that A/J mice are not able to develop long-lasting hydrosalpinx if C5 is required for the conversion of early hydrosalpinx into long-lasting hydrosalpinx. Although complement component 3 (C3) has been shown to be protective in controlling *C. muridarum* lung infection (40), the role of C5 in either chlamydial infection or pathogenesis has not been evaluated. Since C5 can be activated independently of C3 (41), we are currently examining the role of C5 in chlamydial induction of hydrosalpinx, which may help explain the pronounced pathological differences observed between A/J and CBA/J mice and provide insights in devising effective therapeutic interventions.

Although we have revealed a distinct difference in long-lasting hydrosalpinx development between CBA/J and A/J mice, it is not clear whether these two strains also display such a distinct difference in infertility during mating experiments. Thus, besides using the CBA/J and A/J mouse platform to further understand the cellular and molecular mechanisms involved in hydrosalpinx development, it will be worth testing whether A/J mice can also maintain largely normal fertility 60 days after *C. muridarum* infection when CBA/J mice are induced to develop significant infertility.

REFERENCES

1. **Sherman KJ, Daling JR, Stergachis A, Weiss NS, Foy HM, Wang SP, Grayston JT.** 1990. Sexually transmitted diseases and tubal pregnancy. Sex. Transm. Dis. **17:**115–121. http://dx.doi.org/10.1097/00007435-199007000-00001.
2. **de la Maza LM, Pal S, Khamesipour A, Peterson EM.** 1994. Intravaginal inoculation of mice with the Chlamydia trachomatis mouse pneumonitis biovar results in infertility. Infect. Immun. **62:**2094–2097.
3. **Shah AA, Schripsema JH, Imtiaz MT, Sigar IM, Kasimos J, Matos PG, Inouye S, Ramsey KH.** 2005. Histopathologic changes related to fibrotic oviduct occlusion after genital tract infection of mice with Chlamydia muridarum. Sex. Transm. Dis. **32:**49–56. http://dx.doi.org/10.1097/01.olq.0000148299.14513.11.
4. **Murthy AK, Li W, Guentzel MN, Zhong G, Arulanandam BP.** 2011. Vaccination with the defined chlamydial secreted protein CPAF induces robust protection against female infertility following repeated genital chlamydial challenge. Vaccine **29:**2519–2522. http://dx.doi.org/10.1016/j.vaccine.2011.01.074.
5. **Stephens RS.** 2003. The cellular paradigm of chlamydial pathogenesis. Trends Microbiol. **11:**44–51. http://dx.doi.org/10.1016/S0966-842X(02)00011-2.
6. **Cheng W, Shivshankar P, Li Z, Chen L, Yeh IT, Zhong G.** 2008. Caspase-1 contributes to Chlamydia trachomatis-induced upper urogenital tract inflammatory pathologies without affecting the course of infection. Infect. Immun. **76:**515–522. http://dx.doi.org/10.1128/IAI.01064-07.
7. **Cotter TW, Meng Q, Shen ZL, Zhang YX, Su H, Caldwell HD.** 1995. Protective efficacy of major outer membrane protein-specific immunoglobulin A (IgA) and IgG monoclonal antibodies in a murine model of Chlamydia trachomatis genital tract infection. Infect. Immun. **63:**4704–4714.
8. **Pal S, Peterson EM, de la Maza LM.** 2005. Vaccination with the Chlamydia trachomatis major outer membrane protein can elicit an immune response as protective as that resulting from inoculation with live bacteria. Infect. Immun. **73:**8153–8160. http://dx.doi.org/10.1128/IAI.73.12.8153-8160.2005.
9. **Rodgers AK, Budrys NM, Gong S, Wang J, Holden A, Schenken RS, Zhong G.** 2011. Genome-wide identification of Chlamydia trachomatis antigens associated with tubal factor infertility. Fertil. Steril. **96:**715–721. http://dx.doi.org/10.1016/j.fertnstert.2011.06.021.
10. **Chanelles O, Ducarme G, Sifer C, Hugues JN, Touboul C, Poncelet C.** 2011. Hydrosalpinx and infertility: what about conservative surgical management? Eur. J. Obstet. Gynecol. Reprod. Biol. **159:**122–126. http://dx.doi.org/10.1016/j.ejogrb.2011.07.004.
11. **Budrys NM, Gong S, Rodgers AK, Wang J, Louden C, Shain R, Schenken RS, Zhong G.** 2012. Chlamydia trachomatis antigens recognized in women with tubal factor infertility, normal fertility, and acute infection. Obstet. Gynecol. **119:**1009–1016. http://dx.doi.org/10.1097/AOG.0b013e3182519326.
12. **Lei L, Chen J, Hou S, Ding Y, Yang Z, Zeng H, Baseman J, Zhong G.** 2014. Reduced live organism recovery and lack of hydrosalpinx in mice infected with plasmid-free Chlamydia muridarum. Infect. Immun. **82:**983–992. http://dx.doi.org/10.1128/IAI.01543-13.
13. **Darville T, O'Neill JM, Andrews CW, Jr, Nagarajan UM, Stahl L, Ojcius DM.** 2003. Toll-like receptor-2, but not Toll-like receptor-4, is essential for development of oviduct pathology in chlamydial genital tract infection. J. Immunol. **171:**6187–6197.
14. **Chen L, Lei L, Chang X, Li Z, Lu C, Zhang X, Wu Y, Yeh IT, Zhong G.** 2010. Mice deficient in MyD88 develop a Th2-dominant response and severe pathology in the upper genital tract following Chlamydia muridarum infection. J. Immunol. **184:**2602–2610. http://dx.doi.org/10.4049/jimmunol.0901593.
15. **Barteneva N, Theodor I, Peterson EM, de la Maza LM.** 1996. Role of neutrophils in controlling early stages of a Chlamydia trachomatis infection. Infect. Immun. **64:**4830–4833.
16. **Andrew DW, Cochrane M, Schripsema JH, Ramsey KH, Dando SJ, O'Meara CP, Timms P, Beagley KW.** 2013. The duration of Chlamydia muridarum genital tract infection and associated chronic pathological changes are reduced in IL-17 knockout mice but protection is not increased further by immunization. PLoS One **8:**e76664. http://dx.doi.org/10.1371/journal.pone.0076664.
17. **Darville T, Andrews CW, Jr, Sikes JD, Fraley PL, Rank RG.** 2001. Early local cytokine profiles in strains of mice with different outcomes from chlamydial genital tract infection. Infect. Immun. **69:**3556–3561. http://dx.doi.org/10.1128/IAI.69.6.3556-3561.2001.
18. **Imtiaz MT, Schripsema JH, Sigar IM, Kasimos JN, Ramsey KH.** 2006. Inhibition of matrix metalloproteinases protects mice from ascending infection and chronic disease manifestations resulting from urogenital Chlamydia muridarum infection. Infect. Immun. **74:**5513–5521. http://dx.doi.org/10.1128/IAI.00730-06.
19. **Ramsey KH, Sigar IM, Rana SV, Gupta J, Holland SM, Byrne GI.** 2001. Role for inducible nitric oxide synthase in protection from chronic Chlamydia trachomatis urogenital disease in mice and its regulation by oxygen

free radicals. Infect. Immun. **69:**7374–7379. http://dx.doi.org/10.1128/IAI.69.12.7374-7379.2001.

20. **Nagarajan UM, Sikes JD, Yeruva L, Prantner D.** 2012. Significant role of IL-1 signaling, but limited role of inflammasome activation, in oviduct pathology during Chlamydia muridarum genital infection. J. Immunol. **188:**2866–2875. http://dx.doi.org/10.4049/jimmunol.1103461.
21. **Igietseme JU, Omosun Y, Partin J, Goldstein J, He Q, Joseph K, Ellerson D, Ansari U, Eko FO, Bandea C, Zhong G, Black CM.** 2013. Prevention of Chlamydia-induced infertility by inhibition of local caspase activity. J. Infect. Dis. **207:**1095–1104. http://dx.doi.org/10.1093/infdis/jit009.
22. **Chen L, Cheng W, Shivshankar P, Lei L, Zhang X, Wu Y, Yeh IT, Zhong G.** 2009. Distinct roles of CD28- and CD40 ligand-mediated costimulation in the development of protective immunity and pathology during Chlamydia muridarum urogenital infection in mice. Infect. Immun. **77:**3080–3089. http://dx.doi.org/10.1128/IAI.00611-08.
23. **Murthy AK, Li W, Chaganty BK, Kamalakaran S, Guentzel MN, Seshu J, Forsthuber TG, Zhong G, Arulanandam BP.** 2011. Tumor necrosis factor alpha production from CD8+ T cells mediates oviduct pathological sequelae following primary genital Chlamydia muridarum infection. Infect. Immun. **79:**2928–2935. http://dx.doi.org/10.1128/IAI.05022-11.
24. **Cheng W, Shivshankar P, Zhong Y, Chen D, Li Z, Zhong G.** 2008. Intracellular interleukin-1alpha mediates interleukin-8 production induced by Chlamydia trachomatis infection via a mechanism independent of type I interleukin-1 receptor. Infect. Immun. **76:**942–951. http://dx.doi.org/10.1128/IAI.01313-07.
25. **Rasmussen SJ, Eckmann L, Quayle AJ, Shen L, Zhang YX, Anderson DJ, Fierer J, Stephens RS, Kagnoff MF.** 1997. Secretion of proinflammatory cytokines by epithelial cells in response to Chlamydia infection suggests a central role for epithelial cells in chlamydial pathogenesis. J. Clin. Investig. **99:**77–87. http://dx.doi.org/10.1172/JCI119136.
26. **Chen C, Chen D, Sharma J, Cheng W, Zhong Y, Liu K, Jensen J, Shain R, Arulanandam B, Zhong G.** 2006. The hypothetical protein CT813 is localized in the Chlamydia trachomatis inclusion membrane and is immunogenic in women urogenitally infected with C. trachomatis. Infect. Immun. **74:**4826–4840. http://dx.doi.org/10.1128/IAI.00081-06.
27. **Li Z, Lu C, Peng B, Zeng H, Zhou Z, Wu Y, Zhong G.** 2012. Induction of protective immunity against Chlamydia muridarum intravaginal infection with a chlamydial glycogen phosphorylase. PLoS One **7:**e32997. http://dx.doi.org/10.1371/journal.pone.0032997.
28. **Zhong G, Reis e Sousa C, Germain RN.** 1997. Production, specificity, and functionality of monoclonal antibodies to specific peptide-major histocompatibility complex class II complexes formed by processing of exogenous protein. Proc. Natl. Acad. Sci. U. S. A. **94:**13856–13861. http://dx.doi.org/10.1073/pnas.94.25.13856.
29. **Fan T, Lu H, Hu H, Shi L, McClarty GA, Nance DM, Greenberg AH, Zhong G.** 1998. Inhibition of apoptosis in chlamydia-infected cells: blockade of mitochondrial cytochrome c release and caspase activation. J. Exp. Med. **187:**487–496. http://dx.doi.org/10.1084/jem.187.4.487.
30. **Zhong G, Fan P, Ji H, Dong F, Huang Y.** 2001. Identification of a chlamydial protease-like activity factor responsible for the degradation of host transcription factors. J. Exp. Med. **193:**935–942. http://dx.doi.org/10.1084/jem.193.8.935.
31. **O'Connell CM, Ingalls RR, Andrews CW, Jr, Scurlock AM, Darville T.** 2007. Plasmid-deficient Chlamydia muridarum fail to induce immune pathology and protect against oviduct disease. J. Immunol. **179:**4027–4034.
32. **Pellicoro A, Ramachandran P, Iredale JP.** 2012. Reversibility of liver fibrosis. Fibrogenesis Tissue Repair **5**(Suppl 1)**:**S26.
33. **Broeze KA, Opmeer BC, Van Geloven N, Coppus SF, Collins JA, Den Hartog JE, Van der Linden PJ, Marianowski P, Ng EH, Van der Steeg JW, Steures P, Strandell A, Van der Veen F, Mol BW.** 2011. Are patient characteristics associated with the accuracy of hysterosalpingography in diagnosing tubal pathology? An individual patient data meta-analysis. Hum. Reprod. Update **17:**293–300. http://dx.doi.org/10.1093/humupd/dmq056.
34. **Chen L, Lei L, Zhou Z, He J, Xu S, Lu C, Chen J, Yang Z, Wu G, Yeh IT, Zhong G, Wu Y.** 2013. Contribution of interleukin-12 p35 (IL-12p35) and IL-12p40 to protective immunity and pathology in mice infected with Chlamydia muridarum. Infect. Immun. **81:**2962–2971. http://dx.doi.org/10.1128/IAI.00161-13.
35. **Lu C, Zeng H, Li Z, Lei L, Yeh IT, Wu Y, Zhong G.** 2012. Protective immunity against mouse upper genital tract pathology correlates with high IFNgamma but low IL-17 T cell and anti-secretion protein antibody responses induced by replicating chlamydial organisms in the airway. Vaccine **30:**475–485. http://dx.doi.org/10.1016/j.vaccine.2011.10.059.
36. **Tuite A, Elias M, Picard S, Mullick A, Gros P.** 2005. Genetic control of susceptibility to Candida albicans in susceptible A/J and resistant C57BL/6J mice. Genes Immun. **6:**672–682. http://dx.doi.org/10.1038/sj.gene.6364254.
37. **Mashruwala MA, Smith AK, Lindsey DR, Moczygemba M, Wetsel RA, Klein JR, Actor JK, Jagannath C.** 2011. A defect in the synthesis of interferon-gamma by the T cells of complement-C5 deficient mice leads to enhanced susceptibility for tuberculosis. Tuberculosis **91**(Suppl 1)**:**S82–S89. http://dx.doi.org/10.1016/j.tube.2011.10.016.
38. **Copland DA, Hussain K, Baalasubramanian S, Hughes TR, Morgan BP, Xu H, Dick AD, Nicholson LB.** 2010. Systemic and local anti-C5 therapy reduces the disease severity in experimental autoimmune uveoretinitis. Clin. Exp. Immunol. **159:**303–314. http://dx.doi.org/10.1111/j.1365-2249.2009.04070.x.
39. **Durigutto P, Macor P, Ziller F, De Maso L, Fischetti F, Marzari R, Sblattero D, Tedesco F.** 2013. Prevention of arthritis by locally synthesized recombinant antibody neutralizing complement component C5. PLoS One **8:**e58696. http://dx.doi.org/10.1371/journal.pone.0058696.
40. **Bode J, Dutow P, Sommer K, Janik K, Glage S, Tummler B, Munder A, Laudeley R, Sachse KW, Klos A.** 2012. A new role of the complement system: C3 provides protection in a mouse model of lung infection with intracellular Chlamydia psittaci. PLoS One **7:**e50327. http://dx.doi.org/10.1371/journal.pone.0050327.
41. **Ramos TN, Darley MM, Weckbach S, Stahel PF, Tomlinson S, Barnum SR.** 2012. The C5 convertase is not required for activation of the terminal complement pathway in murine experimental cerebral malaria. J. Biol. Chem. **287:**24734–24738. http://dx.doi.org/10.1074/jbc.C112.378364.